Dynamic Responses of DOC and DIC Transport to Different Flow Regimes in a Subtropical Small Mountainous River

Yu-Ting Shih[1], Pei-Hao Chen[1], Li-Chin Lee[1], Chien-Sen Liao[2], Shih-Hao Jien[3], Fuh-Kwo Shiah[4], Tsung-Yu Lee[5], Thomas Hein[6], Franz Zehetner[7], Chung-Te Chang[1], Jr-Chuan Huang[1*]

1. Department of Geography, National Taiwan University, Taipei, Taiwan
2. Department of Civil and Ecological Engineering, I-Shou University, Kaohsiung, Taiwan
3. Department of Soil and Water Conservation, National PingTung University of Science & Technology, PingTung, Taiwan
4. Research Center for Environmental Changes, Academia Sinica, Taipei, Taiwan
5. Department of Geography, National Taiwan Normal University, Taipei, Taiwan
6. Institute of Hydrobiology and Aquatic Ecosystem Management, University of Natural Resources and Life Sciences, Lunz, Austria
7. Institute of Soil Research, University of Natural Resources and Life Sciences, Austria

Submitted to HESS

Corresponding author: Jr-Chuan Huang, email: riverhuang@ntu.edu.tw
Associate Professor, Department of Geography, National Taiwan University, Taipei, Taiwan

Abstract

Transport of riverine dissolved carbon (including DOC and DIC) is a crucial process which links terrestrial and aquatic C storages but is rarely examined in subtropical small mountainous rivers. This study monitored DOC and DIC concentrations on a biweekly basis during non-event flow period and at 3-hour intervals during two typhoons in 3 small mountainous rivers (SMR) in southwestern Taiwan between Jan 2014 and Aug 2016. Two hydrological-associated models: HBV and a three end-member mixing model were applied to determine the quantities of DOC and DIC transport from different flowpaths. The results showed that the annual DOC and DIC fluxes were 2.7-4.8 and 48.4-54.3 ton-C km^{-2} yr^{-1}, which were approximately 2 and 20 times higher than the global mean of 1.4 and 2.6 ton-C km^{-2} yr^{-1}. The DIC/DOC ratio was 14.08, much higher than the mean (1.86) of large rivers worldwide, indicating the high rates of chemical weathering and/or low rates of decomposition in this region. Two typhoons contributed 12-14% of the annual streamflow in only 3 days (about 1.0% of the annual time), whereas 15.0-23.5% and 9.2-12.6% of the annual DOC and DIC flux, respectively, suggested that typhoons play a more important role on DOC transport than DIC transport. End-member mixing model suggested that DOC and DIC export was mainly from surface runoff and deep groundwater, respectively. The unique patterns seen in Taiwan SMRs characterized by high dissolved carbon flux, high DIC/DOC ratio, and large transport by intense storms should be taken into consideration when estimating global carbon budgets.

Keywords: dissolved organic carbon, dissolved inorganic carbon, chemical weathering, Taiwan

Introduction

Transport of riverine dissolved organic and inorganic carbon (DOC and DIC) transport by river systems is an important linkage among atmospheric, terrestrial and oceanic C storages (Meybeck and Vörösmarty, 1999; Battin et al., 2008). Most DIC derived from rock weathering is largely affected by tectonic activities, responsive to climatic change and closely linked to atmospheric CO_2 concentration over geological time scales (Lloret et al., 2011). By contrast, DOC is mainly originated from the decomposition of particulate and dissolved organic matter (POM, DOM), which is closely associated with different organic sources, bacterial degradation and redox. Both, DOC and DIC availability in freshwater ecosystems control dynamics of primary producers and microbial components in aquatic food webs (Maberly and Madssen, 2002; Maberly, et al., 2015; Giesler et al., 2014). Globally, exoreic rivers can annually export 0.21 and 0.38 Pg-C of DOC and DIC to the ocean (Huang et al., 2012). Although the quantity is small compared with terrestrial C storage (about 2300 Pg-C) (Battin et al., 2009; Cole et al., 2007; Ludwig et al., 1998), it has direct effects on downstream ecosystems (Lloret et al., 2013; Atkins et al., 2017). From the compilation of global rivers, large rivers yield approximately 1.4 and 2.6 ton-C km^{-2} yr^{-1} of DOC and DIC, representing 21.0% to 37.5% of the global riverine C export (Meybeck and Vörösmarty, 1999). Much of the variation in river export of DOC and DIC depends upon rock lithology, soil properties, climate, runoff, contact time (or flow velocity), aquatic primary production, UVB exposure and streamwater pH (Wymore et al., 2017).

With the urgent demand for precise global C budget and modeling, a thorough understanding of riverine C response to climatic and anthropogenic changes in different regions is needed (Meybeck and Vörösmarty, 1999). Among the regions, humid tropical/subtropical regions characterized by high productivity and rainfall export large quantities of carbon (Galy et al., 2015; Hilton, 2017), with rivers between latitude 30° N and 30° S transporting 62% of the global DOC to the ocean (Dai et al., 2012). For these systems, rates of export (2.1 and 3.3 ton-C km^{-2} yr^{-1} of DOC and DIC, respectively) are much greater than the global averages (1.4 and 2.6 for DOC and DIC, respectively) (Huang et al., 2012). Thus, the tropical/subtropical regions are hypothesized as the hotspots of DOC and DIC flux (Degens and Ittekkot, 1985; Lyons et al., 2002). However, studies on DOC and DIC transport in this region are rare.

For riverine DOC and DIC transport, the flush hypothesis argued that terrestrial C accumulates in the riparian zone and near-stream hillslopes in non-event flow period and the accumulated C is subsequently flushed by major storms when the water table rises (Mei et al., 2014). Since DOC and DIC have different sources and different transport pathways that are active under different flow regimes, shifts in hydrologic flowpaths would alter the quantity and ratio of DIC: DOC (Walvoord and Striegl, 2007). This has become increasingly important because extreme climate events such as tropical cyclones are projected to become more frequent and intense as a result of global warming (Galy et al., 2015; Heimann and Reichstein, 2008). However, little is known about the processes and their underlying mechanisms of DOC and DIC export to rivers (Atkins et al., 2017). Specifically, the concentration and export of DOC and DIC are hypothesized as being quite different between regular and intense storm periods due to changes in the relative contribution from different flowpaths, but studies up to date provide little information on such shifts of DOC and DIC export.

In this study, we monitored DOC and DIC concentration during non-event flow periods (in biweekly frequency) and during two typhoon events (in a 3-hr interval) at a subtropical small mountainous river in southwestern Taiwan. Based on the analysis of DOC, DIC, and major ions in combination with a hydrological model, HBV and 3 end-member mixing model, we aimed to identify different flowpaths of DOC and DIC transport during in different flow regimes. The objectives are to 1) compare the riverine DOC and DIC in concentration, flux and ratio of DIC/DOC in three small mountainous rivers in Taiwan; 2) understand the role of typhoon events on annual flux; and 3) identify the shifts in sources of DOC and DIC between non-event flow and typhoon period.

Material and method

Study site

The study was conducted at the Tsengwen River in southwestern Taiwan. The Tsengwen River originated from Mt. Dongshui (2,611 m *a.s.l.*, above sea level) has a drainage area of 483 km^2 with a mean terrain slope greater than 50%. The landscape is mainly covered by secondary forests dominated by *Eutrema japonica*, *Areca catechu*, and bamboo with small patches of beetle nut and tea plantations. The annual mean temperature is about 19.8℃ with lowest ones in January (17.8ºC) and highest in July (21.1ºC) (Central Weather Bureau, Taiwan, http://www.cwb.gov.tw). The long-term mean annual rainfall is approximately 3,700 mm yr^{-1}, with approximately 80% occurring from May to October. Tropical cyclones, aka typhoons in Western Pacific, with strong winds and torrential rainfalls, usually lash the area and induce intensive mass movements (e.g. landslides and debris flows) within 2-3 days. These short-term, periodic, extreme events mobilize massive amounts of terrestrial materials to the ocean (Kao et al., 2010; Huang et al., 2017).

Three sampling sites were set up: two at tributaries (T1, T2) and one at the mainstream (M3). The drainage area for T1, T2 and M3 are 11.1, 40.1 and 274.1 km^2, respectively. There is a discharge station at M3 monitored by WRA (Water Resources Agency, Taiwan, http:// www.wra.gov.tw) and 14 auto-recording precipitation stations maintained by CWB (Central Weather Bureau, Taiwan). Land-use pattern in the watershed (Fig. 1) were compiled from aerial photos, satellite imageries, and field surveys during 2004-2006 (National Land Surveying and Mapping Center, 2008). The proportion of agricultural land (i.e., areca and tea plantation) accounted for 14.0 and 23.0% of the area in catchments T1 and T2, but only 7.0% in catchment M3. The legacy of mass movement (i.e., landslide scars) induced by typhoons accounted for 3.0-5.3% of the land area of three catchments.

Sampling and chemical analysis

Streamwater was sampled biweekly between January 2014 and August 2016. Additionally, a high frequency (2-3-hr interval) sampling scheme was applied during two typhoon events (Typhoon Matmo, 2014/07/21 to 2014/07/23 and Typhoon Soudelor, 2015/08/06 to 2015/08/08). We took water samples from a bridge by lowering a set of four 1-L HDPE bottles (high-density polyethylene) into the river. An 1-L bottle of water (unfiltered) was used to measure water temperature, pH and electrical conductivity (EC) in the field. Another bottle water samples were filtered (through pre-weighed and pre-combusted 0.7-μm GF/F filters) and stored at 4℃ in a refrigerator for further analyses of major cations and anions in lab. Approximately 50 mL filtrate was acidified by H_3PO_4 for further measurement of DOC (Analytik Jena multi N/C® 3100 Analyzer) with a detection limit of 4 μg/L. Major anions (Cl^-, NO_3^-, SO_4^{2-}) were analyzed by ion chromatography (IC, Methrom® 886 basic plus) with a detection limit of 0.02 mg L^{-1}. Major cations (Na^+, K^+, Mg^{2+}, Ca^{2+}) were analyzed by ICP-OES (PerkinElmer Inc. - Optima 2100 DV) with a detection limit of 0.02 mg L^{-1}. Using the ion balance method, the DIC (mainly composed by HCO_3^- in neutral and weak alkaline water body) was calculated from the difference between the total dissolved anions ($TZ^- = Cl^- + 2SO_4^{2-} + HCO_3^- + NO_3^-$, in μeq/L) and total dissolved cations ($TZ^+ = Na^+ + K^+ + 2Ca^{2+} + 2Mg^{2+}$, in μeq/L) (Misra, 2012; Zhong et al., 2017). To affirm the estimated DIC through [HCO_3^-], we also determined the DIC of some samples through NDIR method (OI Analitical® Aurora 1030W TOC). The high consistency (R^2=0.93) guaranteed the estimated DIC through [HCO_3^-].

Estimation of DOC and DIC flux

The daily concentration and flux of DOC and DIC were estimated by Load Estimator (LOADEST) using the following equation (Runkel et al., 2004):

$$\ln(F) = a_0 + a_1 ln(Q) + a_2 \ln(Q^2) + a_3 \sin(2\pi \cdot dtime) + a_4 \cos(2\pi \cdot dtime) \qquad \text{Eq. (1)}$$

where F, Q, and *dtime* are the flux (kg km^{-2} d^{-1}), discharge (mm d^{-1}) and Julian day (in decimal form), respectively. In LOADEST, the inputs (Q and Julian day) were decentralized (observation minus average and then divided by the average) to avoid the colinearity (Runkel et al., 2004). The coefficient, a_1 and a_2, are coefficients associated with Q representing the hydrological control. The other coefficients (a_3, a_4) which regulate the seasonal variation can mimic the seasonal change in the concentration and flux. The coefficients in Eq. 1. (a_0, a_1, a_2, a_3, a_4) are estimated by Adjusted Maximum Likelihood Estimation (AMLE, Cohn 1988; Cohn et al., 1992) method built in LOADEST program. The indicator, *NSE* and *Bp* are used for performance measure, The *NSE* (Nash-Sutcliffe efficiency coefficient, Nash and Sutcliffe, 1970) calculates the explained variances and measure the performance as following:

$$NSE = 1 - \frac{\sum_{t=1}^{T}(Q_{s,t} - Q_{o,t})^2}{\sum_{t=1}^{T}(Q_{o,i} - \bar{Q}_o)^2} \qquad \text{Eq. (2)}$$

where, the Q_o and Q_s indicate the observed and simulated streamflow [m^3 s^{-1}] in time step, t, respectively and $\overline{Q_o}$ represents the average of the observed streamflow [m^3 s^{-1}]. The *NSE* ranges from negative infinite to 1.0. The zero and the unity presents the performance is equivalent to expected value and perfectly matches between estimations and observations. The *Bp* shows the yield bias in percent, defined as the estimations minus the observations over the observations. Note that LOADEST is only used for the estimation of annual dissolved carbon fluxes. The event-based fluxes are estimated by flow-weighted method directly, since the sampling frequency is high.

Streamflow Simulation

A conceptual hydrological model, HBV (Hydrologiska Byråns Vattenbalansavdelning model, Parajka et al., 2013) was applied to simulate the daily streamflow and hourly streamflow of the two typhoon events in M3 catchment. The details of the HBV model and streamflow simulation are described in Seibert et al. (2012) and supplementary information I. Briefly, HBV streamflow simulation uses rainfall, temperature, evapotranspiration (estimated by temperature and humidity) to simulate the streamflow and its components. For daily streamflow simulation, the daily rainfall, temperature and relative humidity during 2002-2015 from 14 auto-recording weather stations of CWB were used in our simulations. The evapotranspiration was estimated by Linacre method (Linacre, 1977) through R package of evapotranspiration (Guo et al, 2016). The observed M3 streamflow was then used to adjust the parameters through the *NSE*. The calibrated parameter set of M3 was applied to T1 and T2 using their own climatic inputs to simulate their streamflow. For event simulations, a total of 13 events (during 2005-2015) in M3 were used to calibrate the event-based parameter set. We also affirmed the reliability of the event-based streamflow components derived from the HBV models using the EC, [Cl^-], [Mg^{2+}] and [Ca^{2+}] through a 3-endmember mixing model. All the details and modeling works were referred to supplementary I.

End-member mixing analysis

Conceptually, the streamflow is composed of the rapid surface runoff (*RSR*), subsurface runoff (*SSR*), and deep groundwater (*DG*) during rainstorms. DOC and DIC concentrations collected from streamwater were the mixture from the three runoffs and thus the 3-end-member mixing model is used to estimate the relative contributions of the three runoffs. With the assumption of time-invariant sources (we discussed it in supplementary information II) and mass balance, the sources of DOC and DIC transported by the three flow paths can be represented by the following two equations:

$$1 = [Q]_{RSR,\,i} + [Q]_{SSR,\,i} + [Q]_{DG,\,i} \qquad \text{Eq. (3)}$$

$$[C]_{River,,i} = [C]_{RSR}[Q]_{RSR,,i} + [C]_{SSR}[Q]_{SSR,,i} + [C]_{DG}[Q]_{DG,,i} \qquad \text{Eq. (4)}$$

where, the footnote of *RSR*, *SSR*, and *DG* present the rapid surface runoff, subsurface runoff and deep groundwater, respectively and '*i*' indicates the time step. [*Q*] is the proportion of the corresponding runoff, with the sum of the three should be equal to 1 at any time step. The observed elemental concentration, $[C]_{River,,i}$ in the stream is regarded as the mixing result among $[C]_{RSR}$, $[C]_{SSR}$, and $[C]_{DG}$. The unknown end members can be estimated by the observed and the simulated $[C]_{River,,i}$. The performance of simulated concentration was also evaluated by *NSE*.

Results

Temporal dynamics of DOC and DIC concentration and flux

Most of the observed DOC concentrations of the three sites were less than 200 μM (or 2.4 mg-C L^{-1}) with no prominent seasonality, but rapid increases were observed during the two typhoon events (Fig. 2). The mean DOC concentration of the three sites varied from 48 μM in the dry season to 147 μM in the wet season (May to October), with the annual mean of 137 μM. In contrast, DIC concentrations, varied widely from 1500 to 3500 μM, presented the distinct seasonality. The DIC concentrations were higher in the dry season (November to the next April) and lower in the wet season, with substantial drop during typhoons. The mean DIC concentration of the three sites varied from 2216 μM in the dry season to 1928 μM in the wet season, with the annual mean of 1951 μM (Table 2). Monthly fluxes of DOC and DIC estimated by the LOADEST were satisfactorily with R^2 greater than 0.96, *NSE* of 0.88-098 and *Bp* of 0.4%-6.1% (Table 1). The good performance in flux supports the reliability of estimated DOC and DIC fluxes from the LOADEST. On the other hand, the concentrations of DOC and DIC estimated by LOADEST were not well. The R^2 and *NSE* were 0.51-0.63 and of 0.50-0.59 for DIC, slightly better than DOC with the R^2 and *NSE* of 0.34-0.55 and 0.31-0.55, respectively.

The monthly DOC and DIC fluxes represented a distinct seasonal variation (Fig. 3). In general, the estimated DOC flux was 3.7 ton-C km^{-2} yr^{-1}, with about 95% contributed during the wet season and the rest during the dry season, mostly due to higher discharge in the wet season. The annual DIC flux was approximately 52.1 ton-C km^{-2} yr^{-1}, with approximately 88% from the wet season and the rest from the dry season. A notable low export of DOC and DIC in June and July 2015 during wet season was attributed by that the low rainfall, only 62 and 300 mm $month^{-1}$ without typhoon invasion. Specifically, the variations of DOC and DIC concentrations of T1 and M3 during Matmo and Soudelor were shown (Fig. 4). The dataset of DOC and DIC at site T2 was incomplete and not shown due to a road damage during Soudelor. During events, the DOC concentrations were about 100 μM in low flow periods and it increased rapidly to more than 350 and around 270 μM for T1 and M3 during typhoon, respectively, just before the discharge peaks. After the discharge peaks, the DOC concentration quickly decreased to 100 μM returning to levels prior to the typhoons. The DIC concentration showed an opposite temporal pattern compared to DOC. The DIC concentration was up to 2500 μM in low flow periods; however, as rainstorm begins it gradually decreased with the increase of discharge to only 900 and 1200 μM in T1 and M2, respectively. During the recession period, the DIC concentration gradually increased to 2000 and 1500 μM for T1 and M3, respectively. The recovery of DIC concentration to pre-typhoon levels was much slower than that of DOC concentration. The monthly and event DOC and DIC transport indicated that streamflow is the key factor to the seasonal differences in dissolved carbon flux.

Streamflow components and sources of DIC and DOC

After the calibration with 8 historical events (since 2005-2013), the streamflow simulations of Matmo and Soudelor by HBV agreed well with the observed discharge as indicated by the high NSE values (0.82 and 0.89, respectively). In this modeling approach, rapid surface runoff (*RSR*) contributed approximately 40-50% to the total flow, subsurface runoff (*SSR*) accounted for approximately 25%, and the rest was attributed to deep groundwater (*DG*). The 3-endmember mixing model accompanying with Ca^{2+}, Mg^{2+}, Cl^- and EC were used to evaluate the fractions of different runoffs which performed moderately well, with R^2 values of 0.76, 0.73, 0.36 and 0.68 for Ca^{2+}, Mg^{2+}, Cl^- and EC, respectively (details could be referred to supplementary II).

Through the simple streamflow simulation and validation of its components, the proportions of runoff, DOC and DIC fluxes from the different runoffs were determined (Table 3) and the temporal variation of DOC and DIC fluxes transported by the three runoffs were shown in Fig. 5. The two typhoons accounted for 12% and 14.0% of the annual discharge, which consisted only 1.0% of the two year sampling time (i.e., six days). DOC exported during Typhoon Matmo and Soudelor, were 382.5 kg-C km^{-2} (or 15.0%) and 744 kg-C km^{-2} (23.5%), respectively, of the annual yield. Among the three runoffs, *RSR* was the main contributor delivering approximately 40-48% of DOC export during the typhoon periods, followed by *SSR*, about 37%, while the *DG* only contributed about 20%. For DIC, the two events exported 3999.4 kg-C km^{-2} (9.2%) and 6790.3 kg-C km^{-2} (12.6%) of the annual flux, respectively. The *RSR*, *SSR*, and *DG* transported about 29%, 21%, and 50% of DIC during the two typhoon events. Since *DG* accounted for a low proportion of discharge, the high DIC flux from groundwater was likely attributed to the extreme high DIC concentration. In sum, during typhoon period, the DOC is mainly transported by *RSR* due to the large amount of surface runoff flushing the large DOC storage in land surface, whereas the DIC is considerably transported by *DG* owing to the extremely high DIC concentration in groundwater storage, even though the *DG* flow is small.

Discussion

Dissolved carbon dynamics in Taiwan SMR

Global mean DOC and DIC concentrations of large rivers were 479 and 858 μM, respectively, which were considerably greater than the means of 199 and 408 μM, respectively, for many SMRs around the world (Table 4). However, the global mean annual fluxes of DOC and DIC of large rivers were 1.4 and 2.6 ton-C km^{-2} yr^{-1}, respectively, much lower than means of 2.5 and 7.01 ton-C km^{-2} yr^{-1} for SMRs. In Oceania, which is characterized by high temperature, and abundant rainfall, the mean DOC and DIC concentrations were 399 and 1,781 μM (Huang et al., 2012). Due to high rainfall, the fluxes of DOC and DIC in Oceania were 8.0 and 34.0 ton-C km^{-2} yr^{-1}, much higher than the global means of large rivers and SMRs. While our DOC concentration ranges between the means of global large rivers and SMRs, the DIC concentration was much higher than the global means of both large rivers and SMRs (Table 4). Notably, our lower DOC concentration, but higher flux in the SMRs and Oceania islands suggests greater importance of streamflow on DOC export. On the other hand, the high DIC concentration superimposing the high streamflow lead the extremely high DIC export in Taiwan SMRs.

Globally, DOC is positively correlated with discharge, soil organic carbon (SOC) content, and negatively correlated with slope steepness (Ludwig et al., 1996a; Ludwig et al., 1996b). Another study of global DOC flux indicated that the soil C: N ratio could be a dominant predictor for riverine DOC flux (Aitkenhead and McDowell, 2000). For SOC and slope, Schomakers et al. (2017) reported that the SOC in shallow soils (< 100 cm) was only 2.9±0.6 ton-C ha^{-1} six years after a landslide and it increased to 75.7±5.0 ton-C ha^{-1} after 41 years, being still lower than those of the reference sites (75-150 ton-C ha^{-1}). In general, our SOC content is a little low, but comparable with the Oceania islands, should not fully explain the low riverine DOC concentration in our SMRs. The steep slopes, which result in restricted contact time between infiltrated water and the soils (Ludwig et al., 1996; Hale and McDonnell, 2016), may partly explain the low riverine DOC concentration in SMRs. For aquatic ecosystems, the steep landscape morphology, characterized by fast flows and short water residence times in the stream, limits an intense cycling of dissolved organic matter (DOM) in lotic ecosystems (Stutter et al., 2013). The a little SOC, but high productivity could result in consistent DOC supply and high flow velocities likely leads to low productivity of lotic ecosystems. This could explain the low riverine concentrations in our cases; however, due to abundant precipitation, the DOC fluxes are higher than the global average.

Riverine DIC originated from rock weathering generally increases with increases of temperature, runoff and physical erosion rate (Maher and Chamberlain, 2014). Thus, the DIC concentration in SMRs gradually decreases with the latitude gradient (Table 4). However, the DIC concentrations are greater than 1,000 μM in Oceania islands, which is two times higher than the global average, most likely due to the large physical erosion and very high chemical weathering rates associated to the steep topography, high precipitation and high temperature (West, 2012). In our study, the DIC concentration and flux are 1951 μM and 52.1 ton-C km^{-2} yr^{-1}. The DIC concentration was even as high as the concentration in the karst landscape (characterized by extraordinary high DIC concentrations), Wujiang (Zhong et al., 2017). In addition, high physical erosion rates which would expose fresh rocks enhancing interaction with water also provide conditions favorable for chemical weathering (Larsen et al., 2012; Larsen et al., 2014; Lyons et al., 2005). The unique environmental setting elevates our DIC flux up to 10-fold higher than the global mean of 2.6 ton-C km^{-2} yr^{-1} (Meybeck and Vörösmarty, 1999; Dessert et al., 2003).

The DIC/DOC ratios of the global large rivers, SMRs, and Oceania were 1.86, 2.80, and 4.25, respectively (Table 4). The DIC/DOC ratio could be used for improving the understanding of biogeochemical C processes such as photosynthesis and organic carbon mineralization in streams. DIC is the essential source for autotrophic photosynthesis and DOC for microbial decomposition (Lloret et al., 2011; Atkins et al., 2017). The global mean DIC/DOC ratio is around 1.86, indicating that DOC accounts for 35% of the total dissolved carbon in global large rivers. The DIC/DOC ratio in SMRs around the world is about 2.8, which could be due to: 1. large DIC supply or limited DIC consumption, and 2. limited DOM decomposition. The DIC/DOC ratios in our catchments were 14.08, much higher than those in other rivers of Oceania (4.25) and rarely seen at these ranges across the globe. From the viewpoint of a carbon mass balance, the export of dissolved carbon from SMRs and Oceania islands is contributed mainly from DIC, which is different from that of the global large rivers. Therefore, when discussing global carbon dynamics, the SMRs and Oceania islands accounting for the small relative to global land mass, might have a disproportional dissolved carbon flux, particularly during rainstorms. An important implication is that the dissolved carbon export in SMRs and Oceania islands is sensitive to environmental change (e.g. rainfall intensification and global warming).

Sources of dissolved carbon in different flow regimes

The estimated DOC and DIC transport from different runoffs and the observed concentration-discharge (C-Q) relationships for DOC and DIC were illustrated in Fig. 6. In the C-Q relationship (the plots in the center of the figure), the streamflow enhances the DOC concentration, but dilutes the DIC concentration (e.g. Jin et al., 2014; Battin et al., 2003; Wymore et al., 2017; Zhong et al., 2017). The tighter C-Q relationship for DIC than DOC indicates that the mechanism of DOC transport cannot solely be explained by discharge control, possibly because microbial decomposition also played an important role (Yeh et al., 2018). Based on the source identification using the 3 end-member mixing model, the DOC concentrations of the three sources (*RSR*, rapid surface runoff; *SSR*, subsurface runoff; and *DG*, deep groundwater) were estimated to be 108, 206, and 86 μM, respectively. The source identification and independent validation can be found in supplementary information II. The estimated DOC concentrations in *SSR* and *DG* were one to two orders of magnitude lower than the DOC in *RSR*. Thus, the land surface or the topsoils should be the main source of DOC. In fact, Schomakers et al. (2018) measured the SOC in top soil (0-10 cm) by using ultrasonic-induced soil aggregate breakdown method is between 3.6-11.3 mM and decreases significantly with depth. The much lower estimated DOC concentration in *RSR* possibly could be due to that the ultrasonic-induced soil aggregate breakdown method expels all DOC from the soil, while our estimate only includes DOC transported by *RSR*. Due to the short contact time of water with land surface during extreme events, the DOC might not be disaggregated and transported out to streamwater. On the other hand, the lower DOC concentration in *DG* partly explains the low riverine DOC concentration in the low flow period, since *DG* is the main contributor of baseflow. During high flows, abundant *RSR* and *SSR* rapidly surge and flush terrestrial allochthonous DOC from soils into the stream leading to the enhancement mode in the C-Q relationship, which is consistent with the flush hypothesis (Mei et al., 2014). On the other hand, the DIC concentration increased from 915 to 2,297 μM with increases of soil depth, following the weathering gradient. The much higher DIC concentration in *DG* indicated that weathering likely takes place in the deep rocks (Calmels et al., 2011). Thus, the riverine DIC concentration would be strongly diluted by a large contribution of *RSR* and *SSR* during high flows.

Furthermore, two interesting questions could be addressed. First, what is the main DOC source in stream water during typhoon periods? Some studies suggested that the riparian zone is the main source of DOC during a rainstorm, as described by the flush hypothesis (Winterdahl et al., 2011; Wymore et al., 2017). However, hillslopes, as illustrated in our conceptual model, have also been proven an important source of DOC when rainstorms connect the hillslopes to stream by runoffs (i.e., hydrological connectivity, Birkel et al., 2014). Further researches using isotope techniques,xfor example, ^{13}C of DOM and ^{18}O of different runoffs at different locations along hillslopes may help to clarify the relative importance of riparian zones and hillslopes on DOC export. Another interesting question is the changes in the relative contributions from the three sources between non-event flow periods and extreme storm events in SMRs. Not only the change of DOC concentration, but also the

DOC quality were rapidly changed with the changing flow regimes. For example, Lloret et al. (2011) argued that high water level washed out the lower molecular weight of DOC from the subsurface layer into streams. In our study, one typhoon could transport 12-14% of annual streamflow, with 15-23.5% and 9.2-12.6% of annual DOC and DIC fluxes demonstrating the disproportional DOC and DIC transport by rainstorms. On average, there are 3-6 typhoons per year making landfall to Taiwan (Lin et al., 2017). Thus, the annual DOC and DIC flux contributed by typhoons may be as high as 50% and 30%, respectively. Lloret et al. (2013) reported that flash floods account for 60% of the annual DOC export and 25-45% of the DIC export in small tropical volcanic islands, highlighting the important role of these extreme meteorological events. With the projected global warming, the frequency and intensity of extreme rainfall is expected to increase, while mild rainfall tends to be reduced in Taiwan (Liu et al., 2009). Thus, streamflow may become more variable, scanter in the dry season and higher in the wet season (Huang et al., 2014; Lee et al., 2015). In this regard, the water residence time would be longer in the dry season, which is very likely favorable for autotrophic production and subsequently, DOC accumulation. The accumulated DOC would tend to change the heterotrophic microbes and lower the pH value because of humic acid, enhancing the dissolution/precipitation of carbonate minerals (DIC). By contrast, the intensification of floods and the high flow velocity would destroy the riverbed and reset the aquatic ecosystems, which is unfavorable for heterotrophic microbes. Under such conditions, the difference in DIC/DOC ratio between dry and wet season would be exaggerated with the potential of altering the biogeochemical C processes in aquatic ecosystems.

Conclusions

This study found that although the mean DOC concentrations in SMRs in southwestern Taiwan was as low as 99-174 µM, much lower than the global mean of 479 µM, the DOC flux was very high, 2.7-4.8 ton-C km^{-2} yr^{-1}, 2-3 times the global average of 1.4 ton-C km^{-2} yr^{-1}. The low DOC concentrations is likely attributed to steep landscape morphology which limits the contact time of water with soils. On the other hand, the abundant rainfall still led to the high DOC flux in the SMRs revealing the importance of streamflow control on DOC export. By contrast, DIC concentration and flux are as high as 1805-2099 µM and 48.4-54.3 ton-C km^{-2} yr^{-1}, much higher than the global mean of 858 µM and 2.6 ton-C km^{-2} yr^{-1}. The extreme high DIC concentration and flux resulted from active chemical weathering, representing a high supply for aquatic photosynthesis. From the perspective of global large rivers, the mean DIC/DOC ratio of 1.86 indicated that the DOC accounts for 35% of the total dissolved carbon export. However, our much higher DIC/DOC ratio (14.08) indicates that DOC only accounts for 6.6% of the dissolved carbon, which might not be only unusual in Taiwan, but for other SMRs.

The DOC and DIC fluxes during two typhoon events (accounted for only 1.0% of the annual time) contributed 15-23% and 9.2-12.6% of annual DOC and DIC flux, respectively, highlighting the role of extreme events DOC and DIC transport. The enhancement of DOC during higher streamflow indicates the hillslope or riparian zone could be an important DOC source which was disproportionally flushed out during high flow regime. In contrast, the dilution effect of DIC associated with high streamflow implies that there was a large amount of runoff passed through sources with low DIC (e.g., land surface). The modeling work demonstrated the patterns of DOC and DOC transport were rapidly transferred during high and low flow regimes. The DOC was mainly from the land surface flushed out by surface runoff, whereas the DIC is mainly transported by deep groundwater. However, the linkage of different C storages to streams requires further investigations. Riparian zones and hillslopes, both have been suggested as the major DOC source during rainstorms, but the exact sources and the DOC mobilization and transformation during different flow regimes in SMRs have not been comprehensively addressed. The high dissolved carbon flux, high DIC/DOC ratio, and large transport by rainstorms in SMRs should be considered in estimating global carbon budgets.

Acknowledgement

This study was sponsored by Taiwan Ministry of Science and Technology, (MOST 107-2621-B-002-003-MY3, MOST 106-2116-M-002-020), Austrian Science Fund (FWF I 1396-B16) and NTU Research Center for Future Earth (107L901004). We sincerely thank Prof. Teng-Chiu Lin for proofreading this manuscript and the reviewers for their constructive comments.

Reference

Aitkenhead, J. A., and McDowell, W. H.: Soil C:N ratio as a predictor of annual riverine DOC flux at local and global scales, Global Biogeochem. Cy., 14, 127-138, 10.1029/1999GB900083, 2000.

Alin, S. R., Aalto, R., Goni, M. A., Richey, J. E., and Dietrich, W. E.: Biogeochemical characterization of carbon sources in the Strickland and Fly rivers, Papua New Guinea, Journal of Geophysical Research, 113, 10.1029/2006jf000625, 2008.

Argerich, A., Haggerty, R., Johnson, S. L., Wondzell, S. M., Dosch, N., Corson-Rikert, H., Ashkenas, L. R., Pennington, R., and Thomas, C. K.: Comprehensive multiyear carbon budget of a temperate headwater stream, J Geophys Res-Biogeo, 121, 1306-1315, 10.1002/2015jg003050, 2016.

Atkins, M. L., Santos, I. R., and Maher, D. T.: Seasonal exports and drivers of dissolved inorganic and organic carbon, carbon dioxide, methane and delta13C signatures in a subtropical river network, Sci. Total Environ., 575, 545-563, 10.1016/j.scitotenv.2016.09.020, 2017.

Battin, T. J., Kaplan, L. A., Newbold, J. D., and Hendricks, S. P.: A mixing model analysis of stream solute dynamics and the contribution of a hyporheic zone to ecosystem function, Freshwater Biol, 48, 995-1014, 10.1046/j.1365-2427.2003.01062.x, 2003.

Battin, T. J., Kaplan, L. A., Findlay, S., Hopkinson, C. S., Marti, E., Packman, A. I., Newbold, J. D., and Sabater, F.: Biophysical controls on organic carbon fluxes in fluvial networks, Nat Geosci, 1, 95-100, 10.1038/ngeo101, 2008.

Battin, T. J., Luyssaert, S., Kaplan, L. A., Aufdenkampe, A. K., Richter, A., and Tranvik, L. J.: The boundless carbon cycle, Nat Geosci, 2, 598-600, 10.1038/ngeo618, 2009.

Birkel, C., Soulsby, C., and Tetzlaff, D.: Integrating parsimonious models of hydrological connectivity and soil biogeochemistry to simulate stream DOC dynamics, Journal of Geophysical Research: Biogeosciences, 119, 1030-1047, 10.1002/2013JG002551, 2014.

Calmels, D., Galy, A., Hovius, N., Bickle, M., West, A. J., Chen, M. C., and Chapman, H.: Contribution of deep groundwater to the weathering budget in a rapidly eroding mountain belt, Taiwan, Earth and Planetary Science Letters, 303, 48-58, 10.1016/j.epsl.2010.12.032, 2011.

Calmels, D., Gaillardet, J., and Francois, L.: Sensitivity of carbonate weathering to soil CO2 production by biological activity along a temperate climate transect, Chemical Geology, 390, 74-86, 10.1016/j.chemgeo.2014.10.010, 2014.

Cole, J. J., Prairie, Y. T., Caraco, N. F., McDowell, W. H., Tranvik, L. J., Striegl, R. G., Duarte, C. M., Kortelainen, P., Downing, J. A., Middelburg, J. J., and Melack, J.: Plumbing the global carbon cycle: Integrating inland waters into the terrestrial carbon budget, Ecosystems, 10, 171-184, 2007.

Dai, M., Yin, Z., Meng, F., Liu, Q., and Cai, W.-J.: Spatial distribution of riverine DOC inputs to the ocean: an updated global synthesis, Current Opinion in Environmental Sustainability, 4, 170-178, 10.1016/j.cosust.2012.03.003, 2012.

Degens, E. T., and Ittekkot, V.: Particulate organic carbon an overview, Transport of carbon and minerals in major world rivers, lakes and estuaries. Mitt. Geol.-Palaont. Inst. Univ. Hamburg, 7-27, 1985.

Dessert, C., Dupré, B., Gaillardet, J., François, L. M., and Allègre, C. J.: Basalt weathering laws and the impact of basalt weathering on the global carbon cycle, Chemical Geology, 202, 257-273, https://doi.org/10.1016/j.chemgeo.2002.10.001, 2003.

Freeman, C., Fenner, N., Ostle, N. J., Kang, H., Dowrick, D. J., Reynolds, B., Lock, M. A., Sleep, D., Hughes, S., and Hudson, J.: Export of dissolved organic carbon from peatlands under elevated carbon dioxide levels, Nature, 430, 195-198, 2004.

Galy, V., Peucker-Ehrenbrink, B., and Eglinton, T.: Global carbon export from the terrestrial biosphere controlled by erosion, Nature, 521, 204-207, 10.1038/nature14400, 2015.

Giesler, R., Lyon, S. W., Mörth, C. M., Karlsson, J., Karlsson, E. M., Jantze, E. J., Destouni, G., and Humborg, C.: Catchment-scale dissolved carbon concentrations and export estimates across six subarctic streams in northern Sweden, Biogeosciences, 11, 525-537, 10.5194/bg-11-525-2014, 2014.

Guo, D. L., Westra, S., and Maier, H. R.: An R package for modelling actual, potential and reference evapotranspiration, Environmental Modelling & Software, 78, 216-224, 10.1016/j.envsoft.2015.12.019, 2016.

Hale, V. C., and McDonnell, J. J.: Effect of bedrock permeability on stream base flow mean transit time scaling relations: 1. A multiscale catchment intercomparison, Water Resour. Res., 52, 1358-1374, 10.1002/2014wr016124, 2016.

Heimann, M., and Reichstein, M.: Terrestrial ecosystem carbon dynamics and climate feedbacks, Nature, 451, 289-292, 10.1038/nature06591, 2008.

Hilton, R. G.: Climate regulates the erosional carbon export from the terrestrial biosphere, Geomorphology, 277, 118-132, https://doi.org/10.1016/j.geomorph.2016.03.028, 2017.

Huang, T.-H., Fu, Y.-H., Pan, P.-Y., and Chen, C.-T. A.: Fluvial carbon fluxes in tropical rivers, Current Opinion in Environmental Sustainability, 4, 162-169, 10.1016/j.cosust.2012.02.004, 2012.

Huang, H., Chen, D. J., Zhang, B. F., Zeng, L. Z., and Dahlgren, R. A.: Modeling and forecasting riverine dissolved inorganic nitrogen export using anthropogenic nitrogen inputs, hydroclimate, and land-use change, J. Hydrol., 517, 95-104, 10.1016/j.jhydrol.2014.05.024, 2014.

Huang, J.-C., Milliman, J. D., Lee, T.-Y., Chen, Y.-C., Lee, J.-F., Liu, C.-C., Lin, J.-C., and Kao, S.-J.: Terrain attributes of earthquake- and rainstorm-induced landslides in orogenic mountain Belt, Taiwan, Earth Surface Processes and Landforms, 10.1002/esp.4112, 2017.

Jarvie, H. P., King, S. M., and Neal, C.: Inorganic carbon dominates total dissolved carbon concentrations and fluxes in British rivers: Application of the THINCARB model - Thermodynamic modelling of inorganic carbon in freshwaters, Science of the Total Environment, 575, 496-512, 10.1016/j.scitotenv.2016.08.201, 2017.

Jin, J., Zimmerman, A. R., Moore, P. J., and Martin, J. B.: Organic and inorganic carbon dynamics in a karst aquifer: Santa Fe River Sink-Rise system, north Florida, USA, Journal of Geophysical Research: Biogeosciences, 119, 340-357, 10.1002/2013JG002350, 2014.

Kao, S. J., Dai, M., Selvaraj, K., Zhai, W., Cai, P., Chen, S. N., Yang, J. Y. T., Liu, J. T., Liu, C. C., and Syvitski, J. P. M.: Cyclone-driven deep sea injection of freshwater and heat by hyperpycnal flow in the subtropics, Geophys Res Lett, 37, L21702, 10.1029/2010GL044893, 2010.

Larsen, I. J., and Montgomery, D. R.: Landslide erosion coupled to tectonics and river incision, Nature Geosci, 5, 468-473, http://www.nature.com/ngeo/journal/v5/n7/abs/ngeo1479.html#supplementary-information, 2012.

Larsen, I. J., Almond, P. C., Eger, A., Stone, J. O., Montgomery, D. R., and Malcolm, B.: Rapid Soil Production and Weathering in the Western Alps, New Zealand, Science, 10.1126/science.1244908, 2014.

Lee, T.-Y., Hong, N.-M., Shih, Y.-T., Huang, J.-C., and Kao, S.-J.: The sources of streamwater to small mountainous rivers in Taiwan during typhoon and non-typhoon seasons, Environ Sci Pollut Res, 1-18, 10.1007/s11356-015-5183-2, 2015.

Li, Y.-H.: Denudation of Taiwan Island since the Pliocene Epoch, Geology, 4, 105-107, 10.1130/0091-7613(1976)4<105:DOTIST>2.0.CO;2, 1976.

Lin, K. C., Hamburg, S. P., Wang, L. X., Duh, C. T., Huang, C. M., Chang, C. T., and Lin, T. C.: Impacts of increasing typhoons on the structure and function of a subtropical forest: reflections of a changing climate, Scientific Reports, 7, ARTN 4911, 10.1038/s41598-017-05288-y, 2017.

Linacre, E. T.: A simple formula for estimating evaporation rates in various climates, using temperature data alone, Agricultural meteorology, 18, 409-424, 1977.

Liu, S. C., Fu, C. B., Shiu, C. J., Chen, J. P., and Wu, F. T.: Temperature dependence of global precipitation extremes, Geophys Res Lett, 36, L17702, 10.1029/2009gl040218, 2009.

Lloret, E., Dessert, C., Gaillardet, J., Albéric, P., Crispi, O., Chaduteau, C., and Benedetti, M. F.: Comparison of dissolved inorganic and organic carbon yields and fluxes in the watersheds of tropical volcanic islands, examples from Guadeloupe (French West Indies), Chemical Geology, 280, 65-78, 10.1016/j.chemgeo.2010.10.016, 2011.

Lloret, E., Dessert, C., Pastor, L., Lajeunesse, E., Crispi, O., Gaillardet, J., and Benedetti, M. F.: Dynamic of particulate and dissolved organic carbon in small volcanic mountainous tropical watersheds, Chemical Geology, 351, 229-244, 10.1016/j.chemgeo.2013.05.023, 2013.

Ludwig, W., Suchet, P., Munhoven, G., and Probst, J.-L.: Atmospheric CO2 consumption by continental erosion: Present-day controls and implications for the last glacial maximum, Glob. Planet. Change, 16, 107-120, 10.1016/S0921-8181(98)00016-2, 1998.

Ludwig, W., AmiotteSuchet, P., and Probst, J. L.: River discharges of carbon to the world's oceans: Determining local inputs of alkalinity and of dissolved and particulate organic carbon, Cr Acad Sci Ii A, 323, 1007-1014, 1996a.

Ludwig, W., Probst, J.-L., and Kempe, S.: Predicting the oceanic input of organic carbon by continental erosion, Global Biogeochem. Cy., 10, 23-41, 10.1029/95gb02925, 1996b.

Lyons, T. W., and Berner, R. A.: Carbon-sulfur-iron systematics of the uppermost deep-water sediments of the Black Sea, Chemical Geology, 99, 1-27, https://doi.org/10.1016/0009-2541(92)90028-4, 1992.

Lyons, W. B., Nezat, C. A., Carey, A. E., and Hicks, D. M.: Organic carbon fluxes to the ocean from high-standing islands, Geology, 30, 443-446, Doi 10.1130/0091-7613(2002)030<0443:Ocftto>2.0.Co;2, 2002.

Lyons, W. B., Carey, A. E., Hicks, D. M., and Nezat, C. A.: Chemical weathering in high-sediment-yielding watersheds, New Zealand, Journal of Geophysical Research: Earth Surface, 110, F01008, 10.1029/2003JF000088, 2005.

Maberly, S. C., and Madsen, T. V.: Freshwater angiosperm carbon concentrating mechanisms: processes and patterns, Funct. Plant Biol., 29, 393-405, 2002.

Maberly, S. C., Berthelot, S. A., Stott, A. W., and Gontero, B.: Adaptation by macrophytes to inorganic carbon down a river with naturally variable concentrations of CO2, J. Plant Physiol., 172, 120-127, 10.1016/j.jplph.2014.07.025, 2015.

Maher, K., and Chamberlain, C. P.: Hydrologic Regulation of Chemical Weathering and the Geologic Carbon Cycle, Science, 343, 1502-1504, 2014.

Mei, Y., Hornberger, G. M., Kaplan, L. A., Newbold, J. D., and Aufdenkampe, A. K.: The delivery of dissolved organic carbon from a forested hillslope to a headwater stream in southeastern Pennsylvania, USA, Water Resour. Res., 50, 5774-5796, 10.1002/2014WR015635, 2014.

Meybeck, M., and Vörösmarty, C.: Global transfer of carbon by rivers, Global Change Newsletter, 37, 18-19, 1999.

Parajka, J., Viglione, A., Rogger, M., Salinas, J. L., Sivapalan, M., and Bloschl, G.: Comparative assessment of predictions in ungauged basins - Part 1: Runoff-hydrograph studies, Hydrol. Earth Syst. Sci., 17, 1783-1795, 10.5194/hess-17-1783-2013, 2013.

Runkel, R. L., Crawford, C. G., and Cohn, T. A.: Load estimator (LOADEST): a FORTRAN program for estimating constituent loads in streams and rivers, Report 4-A5, 2004.

Schomakers, J., Jien, S.-H., Lee, T.-Y., Huang, J.-C., Hseu, Z.-Y., Lin, Z. L., Lee, L.-C., Hein, T., Mentler, A., and Zehetner, F.: Soil and biomass carbon re-accumulation after landslide disturbances, Geomorphology, 288, 164-174, http://doi.org/10.1016/j.geomorph.2017.03.032, 2017.

Schomakers, J., Mayer, H., Lee, J.Y., Lee, T.Y., Jien, S.H., Mentler, A., Hein, T., Huang, J.C., Hseu, Z.Y., Cheng, L.W., Yu, C.K., and Zehetner, F.: Soil aggregate breakdown and carbon release along a chronosequence of recovering landslide scars in a subtropical watershed, Catena, 165,

530-536, 2018.
Seibert, J., and Vis, M. J. P.: Teaching hydrological modeling with a user-friendly catchment-runoff-model software package, Hydrol. Earth Syst. Sci., 16, 3315-3325, 10.5194/hess-16-3315-2012, 2012.
Stutter, M. I., Richards, S., and Dawson, J. J.: Biodegradability of natural dissolved organic matter collected from a UK moorland stream, Water Res., 47, 1169-1180, 10.1016/j.watres.2012.11.035, 2013.
Tian, Y. Q., Yu, Q., Feig, A. D., Ye, C., and Blunden, A.: Effects of climate and land-surface processes on terrestrial dissolved organic carbon export to major U.S. coastal rivers, Ecol. Eng., 54, 192-201, 10.1016/j.ecoleng.2013.01.028, 2013.
Walvoord, M. A., and Striegl, R. G.: Increased groundwater to stream discharge from permafrost thawing in the Yukon River basin: Potential impacts on lateral export of carbon and nitrogen, Geophys Res Lett, 34, 2007.
West, A. J.: Thickness of the chemical weathering zone and implications for erosional and climatic drivers of weathering and for carbon-cycle feedbacks, Geology, 40, 811-814, 2012.
Winterdahl, M., Futter, M., Köhler, S., Laudon, H., Seibert, J., and Bishop, K.: Riparian soil temperature modification of the relationship between flow and dissolved organic carbon concentration in a boreal stream, Water Resour. Res., 47, 10.1029/2010wr010235, 2011.
Wymore, A. S., Brereton, R. L., Ibarra, D. E., Maher, K., and McDowell, W. H.: Critical zone structure controls concentration-discharge relationships and solute generation in forested tropical montane watersheds, Water Resour. Res., 53, 6279-6295, 10.1002/2016wr020016, 2017.
Yeh, T.C., Liao, C.S., Chen, T.C., Shih, Y.T., Huang, J.C., Zehetner, F., Hein, T.: Differences in N loading affect DOM dynamics during typhoon events in a forested mountainous catchment. Science of the Total Environment, 633, 81-92, 2018.
Zhong, J., Li, S. L., Tao, F. X., Yue, F. J., and Liu, C. Q.: Sensitivity of chemical weathering and dissolved carbon dynamics to hydrological conditions in a typical karst river, Scientific Reports, 7, ARTN 42944 10.1038/srep42944, 2017.
Zhou, W.-J., Zhang, Y.-P., Schaefer, D. A., Sha, L.-Q., Deng, Y., Deng, X.-B., and Dai, K.-J.: The role of stream water carbon dynamics and export in the carbon balance of a tropical seasonal rainforest, southwest China, PloS one, 8, e56646, 10.1371/journal.pone.0056646, 2013.

Table

Table 1. Performance metrics of estimated DOC and DIC flux at the three sites using LOADEST.

	Site	Sample Number*1	Flux R^2	Flux *Bp**2	Flux *NSE*	Concentration R^2	Concentration *NSE*
DOC	T1	76	0.98	4.1	0.93	0.53	0.41
	T2	64	0.98	1.3	0.97	0.55	0.55
	M3	85	0.96	6.1	0.88	0.34	0.31
DIC	T1	65	0.98	0.4	0.94	0.60	0.58
	T2	42	0.97	3.2	0.95	0.63	0.50
	M3	67	0.97	3.1	0.98	0.51	0.59

*1 Sample number varied among catchments due to differnces in site accessiblility assocaited with road damage caused by typhoons or equipment failure.

*2 *Bp* indicates flux bias in percentage, defined as the estimated minus the observed values over the observed values

Table 2. Concentrations and fluxes of DOC and DIC at the three sites during 2014-2015

Catchment	DOC	DIC	DOC	DIC
	conc. (μM)		flux (ton-C km^{-2} $period^{-1}$)	
Annual				
T1	138	2099	3.5	53.4
T2	174	1951	4.8	54.3
M3	99	1805	2.7	48.4
Average	137	1951	3.7	52.1
Wet season[1]				
T1	150	2097	3.3	46.7
T2	184	1890	4.7	48.6
M3	108	1798	2.5	42.6
Average	147	1928	3.5	45.9
Dry Season				
T1	53	2113	0.2	6.7
T2	55	2672	0.1	5.8
M3	37	1863	0.1	5.9
Average	48	2216	0.1	6.1

[1]. wet and dry season are defined from May to October and November to the next April in Taiwan.

Table 3. The fluxes of DOC and DIC, their contributions to annual fluxes (%) and the relative contributions (%) from three sources (rapid surface runoff, subsurface runoff and deep groundwater) at site M3 during the two typhoon events.

		Q_{sim}	DOC	DIC
		mm/event	kg-C km^{-2}/event	
Typhoon Matmo	Flux	248.4	382.5	3999.4
	Event/Annual	12%	15.0%	9.2%
	Rapid surface runoff	40%	40%	24%
	Subsurface runoff	24%	37%	19%
	Deep groundwater	37%	23%	57%
Typhoon Soudelor	Flux	328.0	744.5	6790.3
	Event/Annual	14%	23.5%	12.6%
	Rapid surface runoff	50%	48%	34%
	Subsurface runoff	25%	37%	22%
	Deep groundwater	25%	15%	44%

Table 4. The mean SMR annual concentrations and fluxes of DOC and DIC across the globe.

	Concentration (μM)		**Flux (ton km^{-2} yr^{-1})**		**DIC/DOC***	
Region	DOC	DIC	DOC	DIC		Ref.
Global	479	858	1.44	2.58	1.86	Meybeck and Vörösmarty, 1999[A]
Small mountainous rivers[B]	199	408	2.5	7.01	2.80	
Subarctic streams	222	279	1.52	2.03	1.34	Giesler et al., 2014
Temperate headwater	-	-	1.7	6.3	3.71	Argerich et al., 2016
Tropical seasonal rainforest	308	500	1.02	2.43	2.38	Zhou et al., 2013
Tropical volcanic islands[L]	75	513	2.5	19.6	6.60	Lloret et al., 2011
Tropical volcanic islands[F]	215	339	5.7	4.8	1.39	Lloret et al., 2011
Southwestern China(Karst)	88	2,472	1.5	41.0	27.30	Zhong et al., 2017
Oceania	399	1,781	8.0	34.0[C]	4.25	Huang et al., 2012
Papua New Guinea	321	1,018	8.9	28.2	3.20	Alin et al., 2008
SE Australia Subtropical rivers	360	1,860	0.44	1.1[D]	10.71-13.38	Atkins et al., 2017
Tseng-Wen River, Taiwan	137	1,951	3.7	52.1	14.08	This study

*DIC/DOC is calculated from either concentration or yield depending on data availability.

[A] the DOC and DIC concentration were reversely calculated from fluxes, the details could be referred to Huang et al. (2012)

[B] the values were the average of the listed studies, but did not include Zhong et al. (2017), due to the specificity of karst landscape

[C] the discharge (1572 mm yr^{-1}) that we used is consistent with the GRDC dataset, but about 10 times higher than the value reported by Huang et al., (2012).

[D] the discharge during the sampling period is only one-third of the long-term average due to the ENSO effect.

[L] and [F] indicate low and high flow conditions, respectively.

Figure

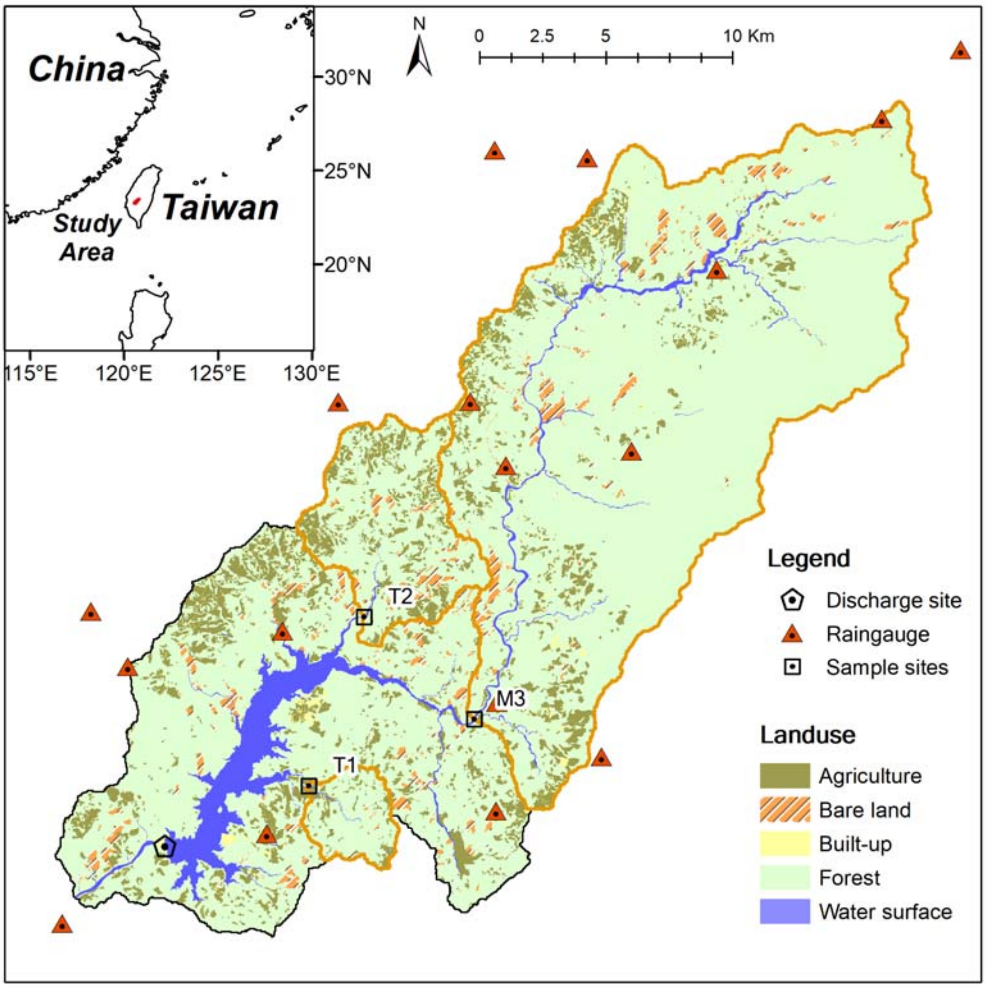

Figure 1. Location map of sampling sites, rain gauges and land cover pattern in Tsengwen catchment**.**

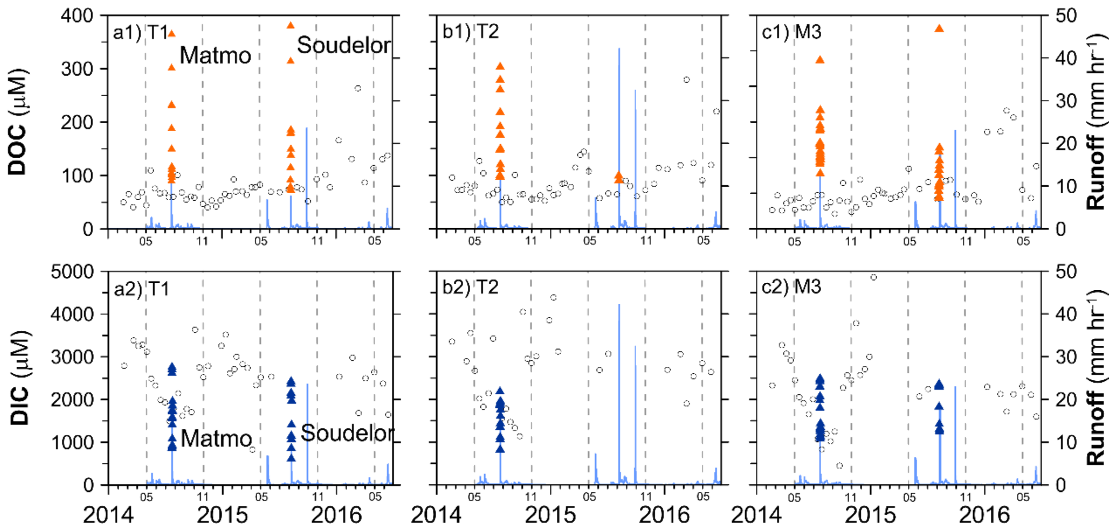

Figure 2. The observed DOC (upper) and DIC (lower) concentration at the three sampling sites (left to right for site T1, T2, and M3) during 2014/01-2016/08. The blue line represents discharge. The black empty circles represent results of biweekly sampling and the orange and blue solid triangles indicate DOC and DIC concentrations during the typhoon events.

646

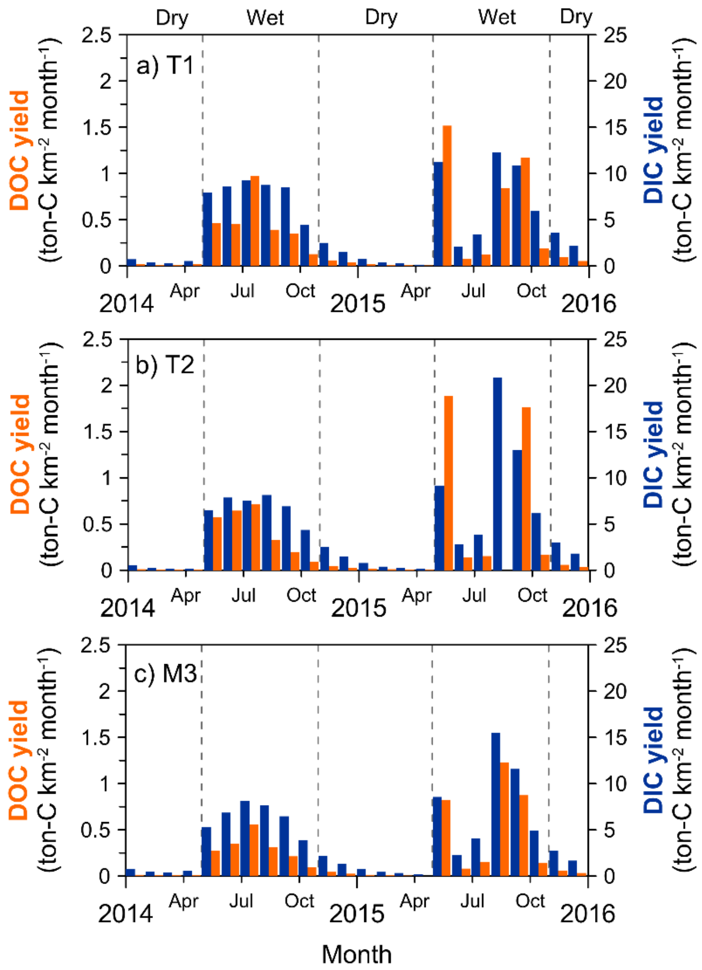

647 **Figure 3.** The DOC and DIC yield (ton C km^{-2} mon^{-1}) at the three sites, T1(a), T2(b) and M3(c).

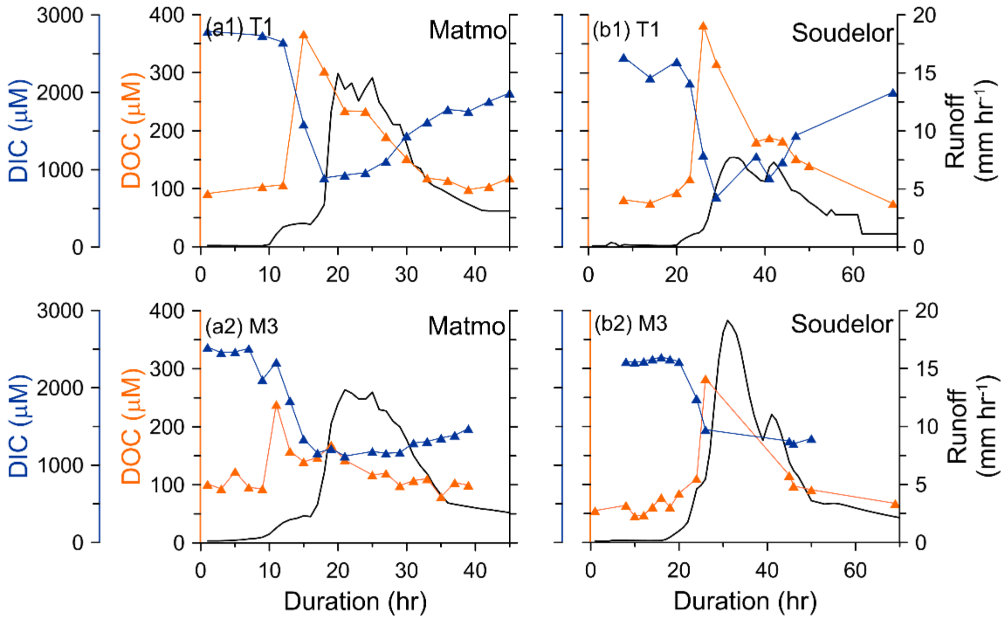

Figure 4. Temporal variation of DOC and DIC concentration during typhoon periods. The left panel is Typhoon Matmo (2014-07-22~2014-07-24) and the right panel is Typhoon Soudelor (2015-08-07~2015-08-10). Upper and lower plots are results of site T1 and M3, respectively.

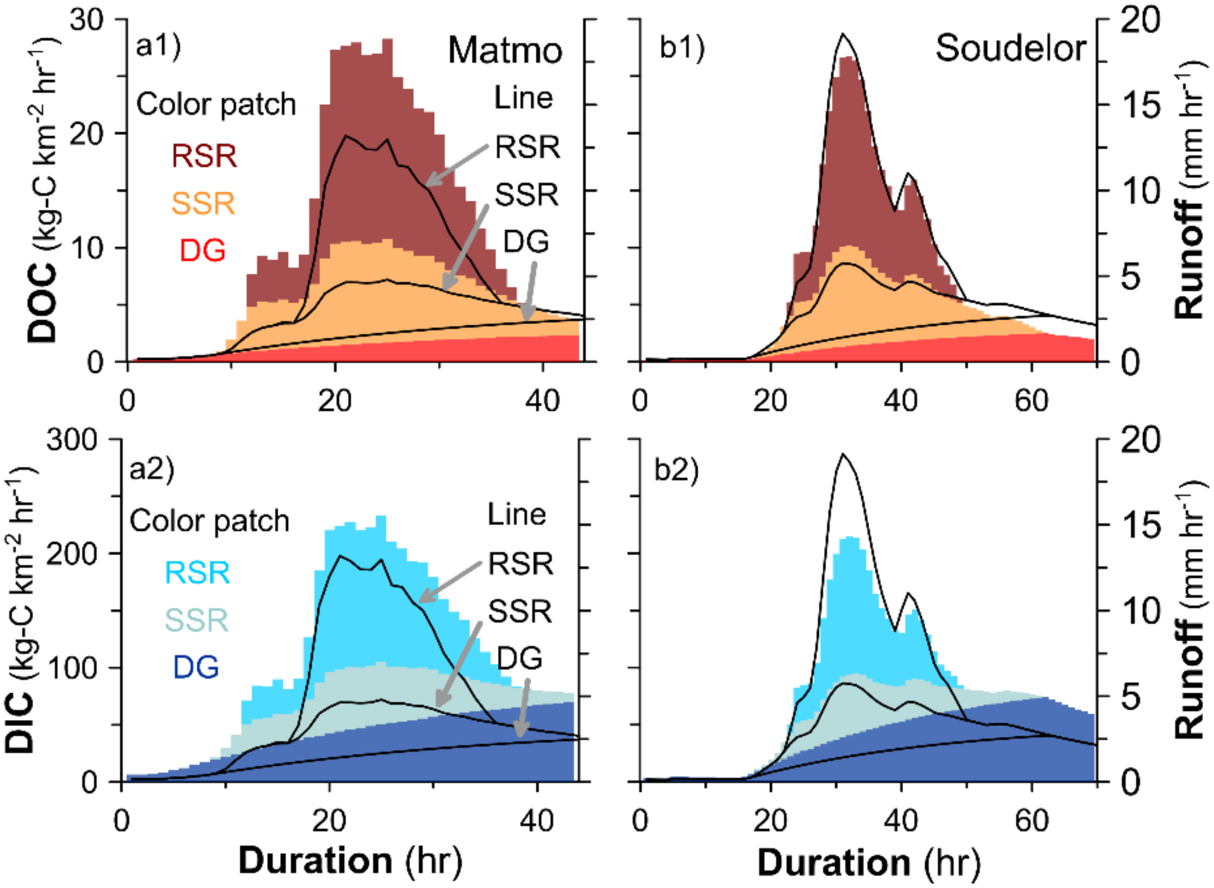

Figure 5. DOC and DIC from different sources during two typhoons at site M3. The colored patches present DOC and DIC flux from RSR (upper patch), SSR (middle patch) and DG (lower patch).The three stacked areas defined by black lines represent the hourly runoff from the three pathways (RSR, SSR and DG, from top to bottom, respectively).

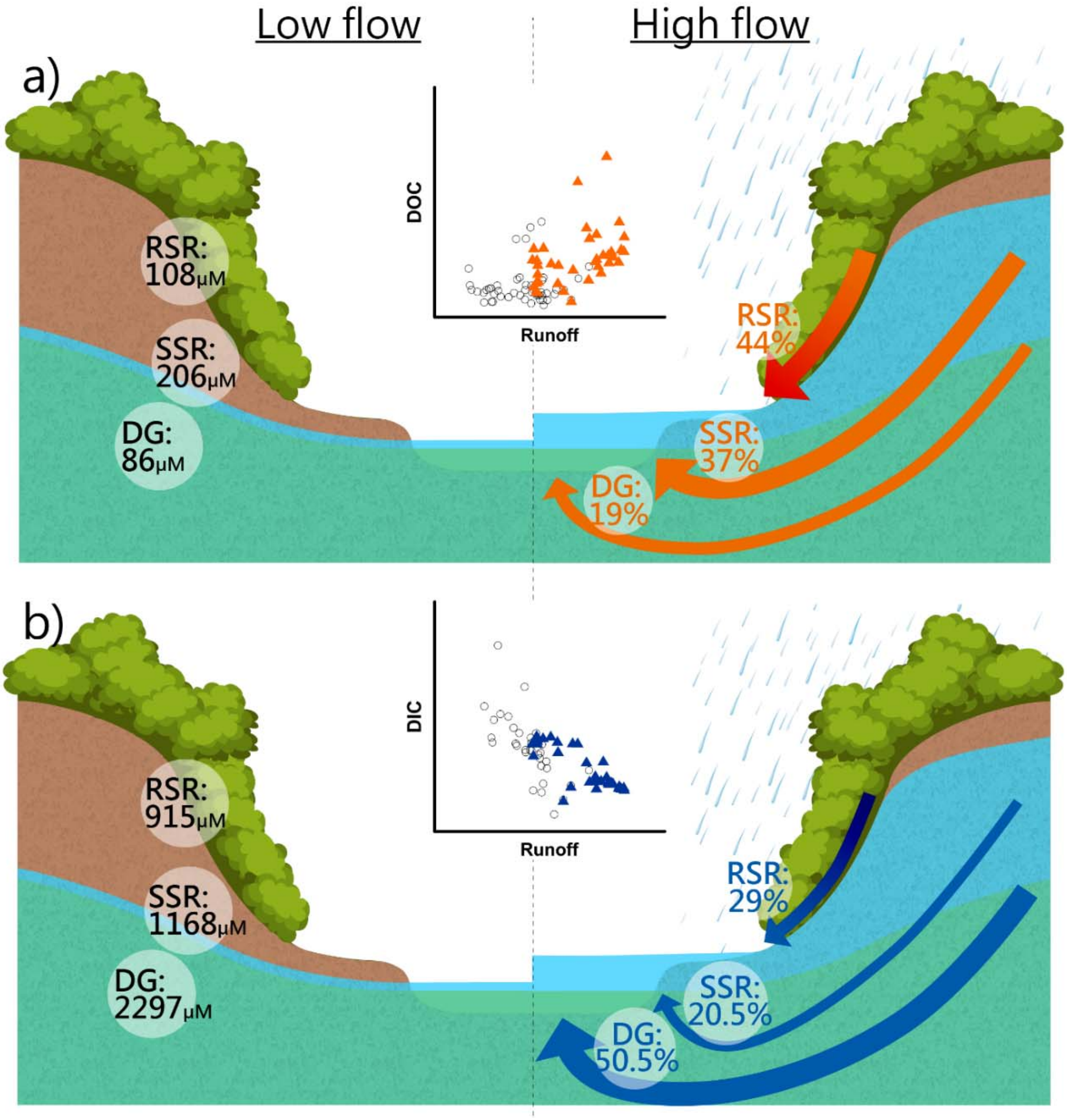

Figure 6. Conceptual model for (a) DOC and (b) DIC transport from different sources at low and high flows. The C-Q relation at low (black circle) and high flows (solid triangle) indicate that higher discharge would enhance DOC and dilute DIC concentrations. The estimated DOC and DIC concentrations from different runoffs are illustrated in the left part. The DOC and DIC concentrations at low flows are consistent with those from DG, since there is no other runoff at low flow regimes. The arrows are in proportion to transport; RSR is the dominant flowpath for DOC transport and DG for DIC at high flows.